Flexibility of single microvilli on live neutrophils and lymphocytes

Da-Kang Yao and Jin-Yu Shao
Department of Biomedical Engineering, Washington University in Saint Louis, Saint Louis, Missouri 63130, USA
(Received 22 February 2007; published 7 August 2007)

We measured the flexural stiffness of single microvilli on live human neutrophils and lymphocytes using 40-nm fluorescent beads. The beads were bound to the tips of the microvilli by anti-*L*-selectin antibodies. Digital bead images were acquired with an exposure time of 3 s at high magnification. Using a Gaussian point spread function, we obtained an analytical expression that relates the image profile to the flexural stiffness. We found that the flexural stiffnesses were 7 and 4 pN/μm for single microvilli on human neutrophils and lymphocytes, respectively. We also verified with live cells that 75% of neutrophil *L*-selectin and 72% of lymphocyte *L*-selectin were on the microvillus tips. Our results indicate that the leukocyte microvilli in contact with the endothelium or other surfaces will bend easily under physiological shear stresses.

DOI: 10.1103/PhysRevE.76.021907 PACS number(s): 87.16.−b, 87.15.La

I. INTRODUCTION

Microvilli are membrane projections on leukocytes, which enable leukocytes to be recruited efficiently from bloodstream to the sites of infection [1]. The leukocyte recruitment is initiated by attachment to the vessel wall followed by leukocyte rolling on the endothelium before firm adhesion and transendothelial migration [2]. Both the attachment and rolling are mediated by *L*-selectin and *P*-selectin glycoprotein ligand-1 (PSGL-1) on leukocytes and *P*- and *E*-selectin on the endothelium. More than 70% of *L*-selectin and PSGL-1 on normal leukocytes are located on the tips of the microvilli [3,4]. The patients with the Wiskott-Aldrich Syndrome suffer from severe immunodeficiency due to fewer microvilli on their leukocytes [5]. The microvilli with concentrated adhesion molecules triple the efficiency of the leukocyte attachment [6]. The microvilli facilitate leukocyte rolling by penetrating into the endothelial glycocalyx, which allow the adhesion molecules on the microvilli access to the ligands on the endothelium [7]. The microvilli can be extended with a spring constant of 43 pN/μm or even elongated into long membrane tubes under physiological shear stress [8]. The extension is believed to stabilize the leukocyte rolling by lowering the pulling force applied on adhesive bonds and prolonging the lifetime of the bonds. However, it is not clear whether the leukocyte microvilli can be bent when the leukocytes attach to and roll on the endothelium in the bloodstream.

The flexibility of leukocyte microvilli has various effects on the leukocyte rolling and intercellular signaling. In vivo leukocytes can roll on the walls of inflamed venules for 86 s and 270 μm before firmly adhering to the endothelium [9]. Slow leukocyte rolling is supported by *E*-selectin and its ligand CD44 [10]. *E*-selectin is expressed on the activated endothelial cells, and CD44 on leukocytes is preferentially excluded from the microvilli and predominantly located on the nonmicrovillar cell body [11]. Microvilli measure about 300 nm on neutrophils and 340 nm on lymphocytes [3,8]. Inflexible microvilli will impede intimate contact between leukocytes and the endothelium and inhibit the bond formation of *E*-selectin with its ligand CD44. In contrast, flexible microvilli may allow the cell-cell body contact and facilitate the bond formation. In addition to the interaction between *E*-selectin and CD44, a variety of cell signaling events occur during the leukocyte rolling, which is necessary for subsequent firm adhesion and transendothelial migration. Many of these cell signaling events are triggered by the binding between the receptors on leukocytes and the ligands on the endothelium, which include at least 19 G protein-coupled chemotactic receptors and 40 chemokines [12]. How effectively these receptors interact with their ligands depends on how easily the leukocyte microvilli can be bent by the physiological shear stress.

In this paper, we examine the flexibility of leukocyte microvilli by measuring the flexural stiffness of single microvilli on live human neutrophils and lymphocytes, which are two major constituents of leukocytes. Our method is modified from one that has been used successfully for measuring the flexural stiffness of carbon nanotubes [13,14]. In that method, the image of a nanotube tip, blurred due to thermal agitation, was matched to the convoluted image computed from the nanotube base image. In our method, 40-nm fluorescent beads were used as probes and bead images were acquired by fluorescence microscopy with an exposure time of 3 s.

II. EXPERIMENT

The experimental setup is shown in Fig. 1. An experimental chamber was affixed firmly on the stage of a Nikon inverted microscope after being filled with 50% autologous plasma with Hanks' balanced salt solution (HBSS; Sigma, St. Louis, MO). The microscope was anchored to a vibration isolation table (TMC, Peabody, MA). A micropipette was inserted into the chamber to hold the cells. The micropipette tip was rested on the chamber bottom, and the micropipette body was glued to the microscope stage. After the fluorescent beads were bound to the microvillar tips of the leukocytes, the cells were injected into the chamber. One spherical cell, on which a fluorescent bead was located and manipulated to the center of the cell bottom, was partially aspirated into the micropipette by a suction pressure. The suction pressure was much less than the threshold pressure capable of causing significant cell deformation [15]. As the cell was

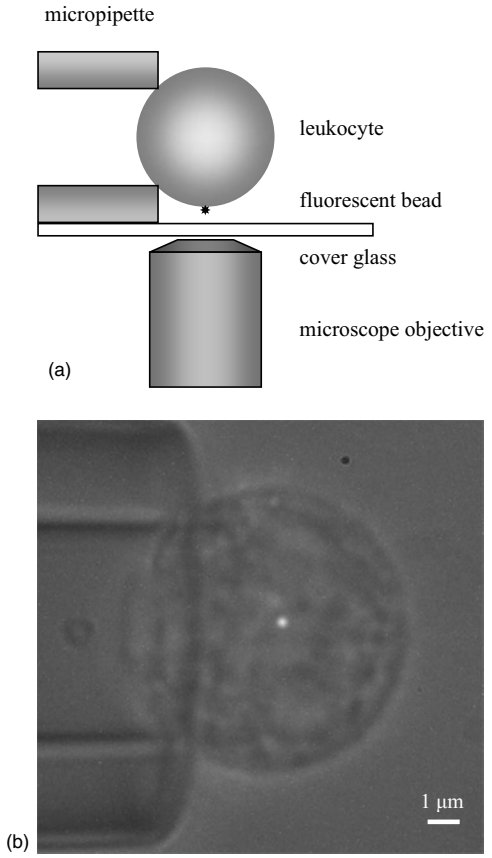

FIG. 1. (a) Schematic of the experimental setup. The leukocyte is held by a micropipette that is immobilized on a cover slip. The fluorescent bead is at the center of the cell bottom and its image is acquired with an exposure time of 3 s. (b) Fluorescent image of a 40-nm bead superposed on a bright field image of a live human leukocyte.

held stationary, the fluorescent bead on the cell bottom was 1–2 μm above the chamber bottom. Fluorescent beads were observed after excitation by a 100-W mercury arc lamp attached to the microscope, which was equipped with an oil immersion 100× Plan-Apo objective (NA=1.4) and a Nikon B-2E/C filter set. Bead images were projected onto a Zeiss digital camera (AxioCam MRm; Carl Zeiss, Thornwood, NY) through a zoom lens (Optem, Fairport, NY). The exposure time of the camera was set to 3 s. For the bead on the bottom of an immobilized cell, each image was collected once the bead was focused. All images were obtained at room temperature (23–25 °C), and the image scale was determined to be 78 pixels per micrometer.

We determined the flexural stiffness of the microvillus by fitting the bead image to its convoluted intensity profile. If the flexural stiffness of the microvillus is K, the potential energy for bending the microvillus is $Kx_i'x_i'/2$ $(i=1,2)$. The bead on the tip of the microvillus is assumed to be in thermal equilibrium. According to Boltzmann's law, the probability density of finding the bead at x_i' is $f(x_i')=K\exp(-Kx_i'x_i'/2\kappa_BT)/2\pi\kappa_BT$, where κ_B is the Boltzmann constant, and T is the absolute temperature. As shown in Fig. 2, the point spread function of the microscope can be approximated as a two-dimensional Gaussian function

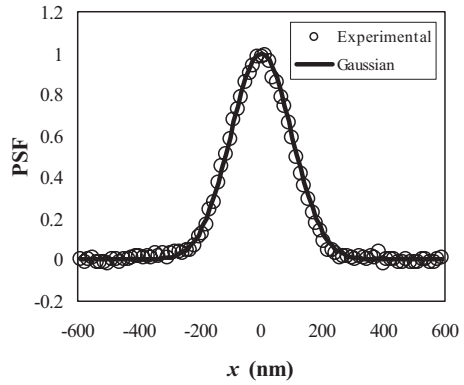

FIG. 2. The point spread function (PSF) of our imaging system. The experimental PSF was measured by averaging 25 images of the beads on eight fixed neutrophils followed by background subtraction and normalization [17]. The images were acquired with an exposure time of 3 s from single 40-nm fluorescent beads, which were bound to fixed neutrophils held by a micropipette immobilized on the bottom of the experimental chamber. The PSF matches the Gaussian distribution very well (correlation coefficient $R^2>0.99$). The width of the PSF (σ_0) is 141 nm.

$G(x_i)=\exp(-x_ix_i/\sigma_0^2)$, where σ_0 is the width of the Gaussian point spread function [16]. By convoluting the Gaussian point spread function with the probability density, the intensity profile of the fluorescent bead on the microvillar tip is expressed as

$$I(r)=\frac{I_0\sigma_0^2}{\sigma_0^2+\sigma^2}\exp\left(-\frac{r^2}{\sigma_0^2+\sigma^2}\right), \tag{1}$$

where I_0 is a constant and

$$\sigma^2=\frac{2\kappa_BT}{K}. \tag{2}$$

The parameter σ_0^2 in Eq. (1) was calibrated by fitting the Gaussian point spread function to the images of the fluorescent nano-beads bound on the bodies of fixed leukocytes. The least-squares method was employed in the fit. The fixed leukocytes were used for *in situ* measurement of the point spread function [17]. The variance σ^2 was obtained by fitting Eq. (1) to the image of the bead bound on the microvillar tip of live cells. In our experiment, we acquired five to nine fluorescent images for each bead by repeating the bead focusing procedure. A total of five to nine variances were obtained after the fit. Three or four variances that were close to each other were averaged to exclude any focusing effect. The flexural stiffness K was calculated from Eq. (2). The accuracy of the variance measurement was estimated by examining ten fluorescent beads immobilized on the fixed cells which were held stationary by the micropipette. The standard deviation of the variances was 240 nm^2, indicating that we were able to measure the flexural stiffness which is smaller than 34 pN/μm.

We prepared samples by isolating, labeling and fixing human neutrophils and lymphocytes. Human blood was obtained from healthy adult donors by finger prick. Neutrophils were isolated by centrifuging a 50-μl sample of fresh blood

layered on 0.2 ml Ficoll-Hypaque density gradient (monopoly resolving medium; MP Biomedicals, Aurora, OH) at $300\times g$ for 15 min at room temperature. Lymphocytes were isolated by centrifuging fresh blood samples of 50 μl on 0.2 ml Histopaque-1077 (Sigma) at $300\times g$ for 10 min at room temperature. The leukocytes were labeled by neutravidin-coated yellow-green fluorescent beads of 40 nm in diameter (Molecular Probes, Eugene, OR), which emit at 519 nm after excitation at 488 nm. The beads were bound to neutrophils or lymphocytes by biotinylated monoclonal mouse anti-human-CD62L (Ancell, Bayport, MN) or anti-human-CD44 (BD Pharmingen, San Diego, CA). BlockAid™ blocking solution (Molecular Probes) was used to suppress nonspecific binding. For microvillus labeling, neutrophils and lymphocytes were incubated in 1 ml of BlockAid™ blocking solution with 0.02 and 0.01 μg of biotinylated anti-CD62L for 10 min at room temperature, respectively. Subsequently, the cells were incubated in 1 ml of the blocking solution with 2 μg of neutravidin-coated fluorescent beads for 30 min at room temperature. For nonmicrovillar cell body labeling, the cells were incubated in the same manner but first with 2 μl of biotinylated anti-CD44 and then with 5 μg of the neutravidin-coated beads. On average, eight bound fluorescent beads per neutrophil and six bound fluorescent beads per lymphocyte were observed after the microvillus labeling. Without the biotinylated antibodies, only two bound beads were found on 50 cells. Thus the binding of the fluorescent beads to neutrophils or lymphocytes was highly specific. Following the cell body labeling, the cells were fixed in 10% formaldehyde (Sigma) for 10 min at 4 °C. Subsequently, the cells were incubated in HBSS at room temperature for 1 h with 1% glycine (Sigma) to quench unreacted formaldehyde, and with 0.02% Alexa Fluor 546 phalloidin (Molecular Probes) to mark the cells. The marker, which emits at 570 nm after excitation at 556 nm, was used to distinguish fixed cells from live cells. Besides fixing the cells, formaldehyde cross-linked the anti-CD44-coated beads covalently to the cell surface. Therefore, those beads on the fixed cells were considered affixed tightly to the cell bodies.

III. RESULTS AND DISCUSSION

The circular symmetry of the bead images was examined by fitting the intensity profiles of the images to an exponential function derived for an imaginary elliptically shaped image [similar to Eq. (1) but with an elliptical exponent]. We calculated the relative difference between the semimajor and semiminor axes of the ellipse. The relative differences were mostly less than 4% for these fluorescent beads, indicating that the images of these beads have very good circular symmetry. In total, we analyzed 217 fluorescent beads on live human neutrophils and 120 fluorescent beads on live human lymphocytes. The variances (σ^2) were obtained by fitting Eq. (1) to the images of these fluorescent beads. The histogram of the variances of the beads is shown in Fig. 3(a) for live neutrophils, and in Fig. 3(b) for live lymphocytes. Both histograms show the distribution of two populations of the variances. The first population concentrates near zero variance,

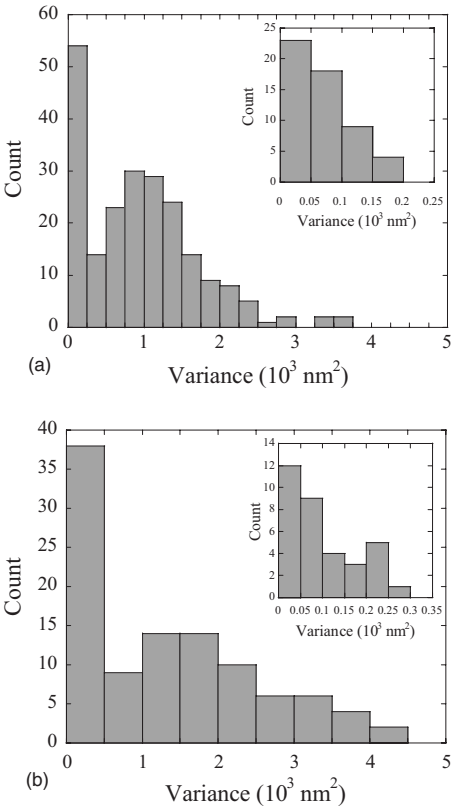

FIG. 3. (a) Histogram of the variances (σ^2) of the beads on live neutrophils. The bin width is 250 nm^2. The bin width in the inset is 50 nm^2. (b) Histogram of the variances (σ^2) of the beads on live lymphocytes. The bin width is 500 nm^2. The bin width in the inset is 50 nm^2.

and the second population spreads along the variance axis. This distribution is consistent with the distribution of *L*-selectins on leukocytes. *L*-selectin is expressed on either the microvillus tip or the cell body of a neutrophil or lymphocyte [18]. About 78% of neutrophil *L*-selectin and 71% of lymphocyte *L*-selectin are located on the microvillus tips [3,18]. We bound the fluorescent beads to the live leukocytes by anti-*L*-selectin. Consequently, the majority of anti-*L*-selectin-coated fluorescent beads should settle on the microvillar tips, and the minority on the cell bodies. The thermal motion of the attached beads on the microvillar tips is larger than the ones on the cell bodies, so the variances of the former are larger than those of the latter. In Fig. 3, the first population with smaller variances was considered to be from the cell bodies and the second from the microvillar tips. The insets in Fig. 3 show that 54 beads were on the bodies of neutrophils and 34 beads were on the bodies of lymphocytes. About 75% of the beads bound to live neutrophils and 72% of the beads bound to live lymphocytes via anti-*L*-selectin were found on the microvilli. This finding is in good agreement with the results in the literature [3,18].

The flexural stiffness of the microvilli was determined by substituting the variances of the second population into Eq. (2). Figure 4(a) shows the distribution of the flexural stiffness of 163 microvilli on live human neutrophils. Figure 4(b) shows the distribution of the flexural stiffness of 86 microvilli on live human lymphocytes. By Poisson fitting, we

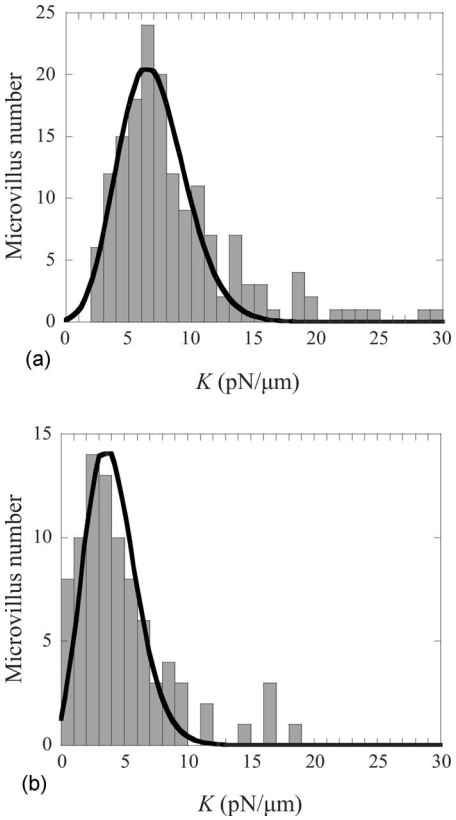

FIG. 4. (a) Histogram of the flexural stiffness (K) of the microvilli on live human neutrophils. The solid curve is a Poisson fit with a mean of 7 pN/μm and an SD of 3 pN/μm (correlation coefficient $R \approx 0.94$). The bin width is 1 pN/μm. (b) Histogram of the flexural stiffness (K) of the microvilli on live human lymphocytes. The solid curve is a Poisson fit with a mean of 4 pN/μm and an SD of 2 pN/μm (correlation coefficient $R \approx 0.93$). The bin width is 1 pN/μm.

found that the flexural stiffness was 7 ± 3 pN/μm (mean ± SD) for individual microvilli on human neutrophils, and 4 ± 2 pN/μm (mean ± SD) for lymphocytes. Lymphocytes are grouped into T cells, B cells, and natural killer cells according to their functions, but they are otherwise morphologically indistinguishable. Hence we measured the flexural stiffness of the microvilli on human lymphocytes without any consideration for their subpopulations. Our measurements show that the microvilli on the leukocytes are so flexible that a small force of a few piconewtons can bend a microvillus easily.

Leukocyte microvilli can be easily bent by physiological hemodynamic forces in the blood vessels where leukocytes circulate. As leukocytes attach to and roll on the endothelium in the venules, the physiological force exerted on the leukocytes from the bloodstream can be as large as 200 pN [19,20], which is large enough to deflect dozens of microvilli. On average, there are five microvilli per μm^2 on neutrophil surface and three microvilli per μm^2 on lymphocyte surface [8,21]. When a leukocyte attaches to or rolls on the endothelium, only several microvilli contact the endothelium [22]. Under the physiological force, these microvilli in contact with the endothelium will flex easily, thereby facilitating access of the receptors on the nonmicrovillar cell body to their ligands on the endothelium.

In our experiments, the exposure time used for acquiring bead images has to be long enough to allow adequate sampling of fluorescent bead positions. At the same time, the exposure time must also be short enough to avoid the photobleaching effect and the possible dynamics of microvilli. To determine the appropriate exposure time, we experimented with two exposure times: 20 and 3 s. We found that the flexural stiffness distributions obtained with the two exposure times are similar (no significant difference found by Student's t test, $p > 0.8$). This finding shows that the 3-s exposure time was long enough for sampling bead positions. Therefore, the 3-s exposure time was chosen. With this exposure time, as many as nine images could be collected from one bead without noticeable photobleaching. In addition to photobleaching, another concern in our study was the possibility of microvillus dynamics during the acquisition of the images [23]. By means of scanning ion conductance microscopy, microvilli have been observed cycling between formation and retraction on toad kidney epithelial cells, human colon cancer cells, murine melanocytes, and fibroblasts [24]. The cycle duration was ~12 min with a stationary period of ~5 min. If the microvilli on human neutrophils and lymphocytes are capable of the same dynamic behavior, this could lead to monotonic increase (during formation) or decrease (during retraction) in the variances we measured. However, from the nine sequential measurements of any one microvillus in our study, no such monotonic changes were observed. Therefore, our observations support the hypothesis that neutrophil and lymphocyte microvilli are relatively stable or change quite slowly within our chosen exposure time.

The effects of bead diffusion and the microvillar extension are negligible in our measurements. To assess the effect of bead diffusion, we measured the diffusion of 31 beads adherent on live leukocytes by single particle tracking [25]. After a live cell was held by the micropipette, a sequence of fluorescent images ($n=21$) of a fluorescent bead, which was located at the center of cell bottom, were taken with an exposure time of 3 s for each image. The positions of the bead were determined by Gaussian fitting. An average diffusion coefficient of 2.0 ± 0.8 nm^2/s (mean ± SD) was found, indicating that the bead diffusion was very little during the 3-s exposure time in our flexural stiffness experiments. This weak bead diffusion is expected because multiple linkages between the bead and cell were highly likely in our experiments. We found with Monte Carlo simulation that the bead diffusion with the diffusion coefficient of 2–10 nm^2/s had little effect on the measurements for the flexural stiffness. The extensional stiffness of neutrophil microvilli is 43 pN/μm at small loading rates [8]. With this extensional stiffness, the fluctuation caused by thermal agitation in the long-axis direction of the microvillus can be estimated to be ~10 nm, which cause little change in the bead focus. At large force loading rates, the extensional stiffness is even larger [26], so the fluctuation in this direction contributes little to the uncertainty in our flexural stiffness measurement.

We can estimate the Young's moduli of the microvilli on neutrophils and lymphocytes from their flexural stiffnesses. If the microvillus is modeled as a continuous, isotropic, and

homogeneous Hookean cylinder, its flexural stiffness is related to the Young's modulus (E) as follows:

$$K = \frac{3\pi}{4}\frac{ER^4}{L^3}, \tag{3}$$

where R is the microvillus radius and L is its length. The average microvillus length is 0.29 μm on neutrophils and 0.34 μm on lymphocytes [3]. If the microvillus radius is assumed to be 0.1 μm [8], the Young's modulus can be calculated from Eq. (3) to be about 724 pN/μm^2 for the neutrophil microvilli and 667 pN/μm^2 for the lymphocyte microvilli. According to these Young's moduli, the flexural stiffnesses for longer microvilli (0.5 μm) on neutrophils and lymphocytes are 1.4 and 1.3 pN/μm, respectively. In comparison, the extensional stiffness of neutrophil microvilli is 43 pN/μm [8]. With the aforementioned microvillus model, the extensional stiffness of the microvilli is related to the Young's modulus as follows:

$$K_E = E\frac{\pi R^2}{L}. \tag{4}$$

From Eq. (4), the Young's modulus of the neutrophil microvilli is calculated to be 397 pN/μm^2. Although the microvillus structure may be much more complicated than our microvillus model, the Young's modulus of the microvilli obtained from the flexural stiffness is in reasonable agreement with that calculated from the extensional stiffness, for which 43 pN/μm may only be an underestimate.

The membrane projections on leukocytes include both fingerlike microvilli and ridgelike ruffles. For the ruffles, which resemble a collection of fingerlike microvilli, their flexural rigidity is larger due to its large cross-sectional area. Therefore, the ruffles should be much stiffer than single microvilli. Our method can only be used to measure the flexural stiffness that is smaller than 34 pN/μm. It is very likely that the flexural stiffness of the ruffles is larger than 34 pN/μm, so the ruffles might have been categorized into the first population in Fig. 3, which was interpreted as the cell-body population in this paper. That may be why the majority of the bead images we acquired are radially symmetrical. There were indeed a few bead images that were asymmetrical (less than five out of all the beads analyzed), i.e., the difference between the semimajor axis and the semiminor axis was larger than 5%. These few beads were excluded from the data analysis.

IV. SUMMARY

We measured the flexural stiffness of individual microvilli on live human neutrophils and lymphocytes. On average, the flexural stiffness of single microvilli was 7 pN/μm for neutrophils and 4 pN/μm for lymphocytes. Our data show that leukocyte microvilli can be easily bent when leukocytes attach to and roll on the endothelium during the leukocyte recruitment. Our method was developed from that used for measuring the flexural stiffness of carbon nanotubes [13,14], which relies on electron microscopy. We used fluorescence microscopy and 40 nm fluorescent beads as probes, and utilized a long exposure time to acquire bead images. We fitted a simple analytical expression to the bead images to determine the flexural stiffness. Although flexural stiffness has been measured for many subcellular structures such as actin filaments and microtubules, to our knowledge, no other method has been applied to any subcellular structure on a live cell such as a leukocyte microvillus. The method in this paper should have great potential in the study of the flexural stiffness of soft subcellular structures and biological macromolecules.

ACKNOWLEDGMENTS

We thank Dr. Salvatore P. Sutera for his critical reading and editing of the manuscript. This work was supported by the National Institutes of Health (R01 HL069947).

[1] C. Korn and U. S. Schwarz, Phys. Rev. Lett. **97**, 138103 (2006).
[2] T. A. Springer, Cell **76**, 301 (1994).
[3] R. E. Bruehl, T. A. Springer, and D. F. Bainton, J. Histochem. Cytochem. **44**, 835 (1996).
[4] K. L. Moore, K. D. Patel, R. E. Bruehl, F. Li, D. A. Johnson, H. S. Lichenstein, R. D. Cummings, D. F. Bainton, and R. P. McEver, J. Cell Biol. **128**, 661 (1995).
[5] L. Westerberg, M. Larsson, S. J. Hardy, C. Fernandez, A. J. Thrasher, and E. Severinson, Blood **105**, 1144 (2005).
[6] J. V. Stein, G. Cheng, B. M. Stockton, B. P. Fors, E. C. Butcher, and U. H. von Andrian, J. Exp. Med. **189**, 37 (1999).
[7] Y. Zhao, S. Chien, and S. Weinbaum, Biophys. J. **80**, 1124 (2001).
[8] J.-Y. Shao, H. P. Ting-Beall, and R. M. Hochmuth, Proc. Natl. Acad. Sci. U.S.A. **95**, 6797 (1998).
[9] E. J. Kunkel, J. L. Dunne, and K. Ley, J. Immunol. **164**, 3301 (2000).
[10] Y. Katayama, A. Hidalgo, J. Chang, A. Peired, and P. S. Frenette, J. Exp. Med. **201**, 1183 (2005).
[11] B. P. Fors, K. Goodarzi, and U. H. von Andrian, J. Immunol. **167**, 3642 (2001).
[12] T. S. Olson and K. Ley, Am. J. Physiol. Regulatory Integrative Comp. Physiol. **283**, R7 (2002).
[13] M. M. J. Treacy, T. W. Ebbesen, and J. M. Gibson, Nature (London) **381**, 678 (1996).
[14] A. Krishnan, E. Dujardin, T. W. Ebbesen, P. N. Yianilos, and M. M. J. Treacy, Phys. Rev. B **58**, 14013 (1998).
[15] E. Evans and A. Yeung, Biophys. J. **56**, 151 (1989).
[16] Y. M. Wang, J. O. Tegenfeldt, W. Reisner, R. Riehn, X. J. Guan, L. Guo, I. Golding, E. C. Cox, J. Sturm, and R. H. Austin, Proc. Natl. Acad. Sci. U.S.A. **102**, 9796 (2005).
[17] J. G. McNally, T. Karpova, J. Cooper, and J. A. Conchello, Methods **19**, 373 (1999).

[18] S. L. Erlandsen, S. R. Hasslen, and R. D. Nelson, J. Histochem. Cytochem. **41**, 327 (1993).
[19] G. W. Schmid-Schoenbein, Y. C. Fung, and B. W. Zweifach, Circ. Res. **36**, 173 (1975).
[20] S. D. House and H. H. Lipowsky, Circ. Res. **63**, 658 (1988).
[21] S. Majstoravich, J. Zhang, S. Nicholson-Dykstra, S. Linder, W. Friedrich, K. A. Siminovitch, and H. N. Higgs, Blood **104**, 1396 (2004).
[22] Y. Yu and J. Y. Shao, Biophys. J. **92**, 418 (2007).
[23] N. S. Gov, Phys. Rev. Lett. **97**, 018101 (2006).
[24] J. Gorelik, A. I. Shevchuk, G. I. Frolenkov, I. A. Diakonov, M. J. Lab, C. J. Kros, G. P. Richardson, I. Vodyanoy, C. R. W. Edwards, D. Klenerman, and Y. E. Korchev, Proc. Natl. Acad. Sci. U.S.A. **100**, 5819 (2003).
[25] M. J. Saxton and K. Jacobson, Annu. Rev. Biophys. Biomol. Struct. **26**, 373 (1997).
[26] E. Evans, V. Heinrich, A. Leung, and K. Kinoshita, Biophys. J. **88**, 2288 (2005).